Bioresource Technology Reports 21 (2023) 101375

Contents lists available at ScienceDirect

Bioresource Technology Reports

journal homepage: www.sciencedirect.com/journal/bioresource-technology-reports

Enhancement of azo dye bioremediation using chemically modified polypropylene biocarrier: Comparative analysis and kinetic modeling

Kanhaiya Lal Maurya [a], Mohit Kumar [a], Ravi Kumar Sonwani [a,b], Vivek Kumar Jaiswal [a], Ankur Verma [a], Ram Sharan Singh [a,*]

[a] Department of Chemical Engineering & Technology, Indian Institute of Technology (BHU), Varanasi 221005, Uttar Pradesh, India
[b] Department of Chemical Engineering, Indian Institute of Petroleum and Energy (IIPE), Visakhapatnam, Andhra Pradesh 530003, India

ARTICLE INFO

Keywords:
Acid blue 113
Chemical modification
Polypropylene
D-optimal design
Moving bed biofilm reactor
Kinetic modeling

ABSTRACT

The present study focused on the surface modification of conventional polypropylene (PP) biocarrier via chemical oxidation and calcium coating for the azo dye degradation. The chemical treatment resulted in the hydrophobic PP (contact angle of 94°) into a hydrophilic material (contact angle of 70°), which ultimately enhanced the bacterial adhesion. In addition, the batch study revealed that the quantity of fixed biomass and the extracellular polymeric substance secretion was increased by 1.51 and 2.13 times, respectively, in the case of the modified biocarrier (i.e., KMNO4-Ca-PP). The performance of the biocarriers for Acid blue 113 dye removal was studied in moving bed biofilm reactor (MBBR) systems by optimizing process parameters, namely dye concentration and hydraulic retention time. The modified biocarriers filled MBBR showed maximum dye removal efficiency of 83.75 % at optimized conditions. Moreover, the modified Stover-Kincannon and Monod models were well fitted with the experimental values.

1. Introduction

The rapid growth of textile industries leads to the discharge of a large volume of wastewater into the aquatic bodies, which causes serious environmental concerns worldwide. The textile industries consume approximately 200 m^3 of freshwater to produce 1.0 t of fabric materials (Barathi et al., 2020). Mostly, azo dyes are extensively used due to their wide coloring ability, excellent binding nature with the fabrics, and minimum cost for bulk production (Emadi et al., 2022; Giri et al., 2020; Maurya et al., 2022). Almost 10–15 % of azo dyes are discharged into the environment along with effluent, which imposes various adverse health and safety issues on the ecosystem (Khan et al., 2021). The persistent nature of the synthetic dyes reduces the dissolved oxygen of the lake and sunlight penetration, which ultimately hinders the growth of aquatic plants and animals (Rosu et al., 2018; Joshi et al., 2020). In addition, the chronic effect of the toxic dye causes dysfunction of the nervous system, eczema, and cancer to the human beings (Tian et al., 2021; Kapoor et al., 2021). Therefore, it becomes a concern for the environmentalist to make an effective and low-cost technology to treat dye-contaminated wastewater. Bioremediation using microorganisms (bacteria, yeast, or fungi) is considered a more energy-efficient and cost-effective technique than the conventional physio-chemical and advanced oxidation processes (Mishra and Maiti, 2018). Complete mineralization of the persistent pollutants, minimum toxic sludge generation, and energy cost are the advantages of the bioremediation technique (Thangaraj et al., 2022; Zhu et al., 2022).

Several bioreactors (i.e., internal airlift bioreactor, moving bed biofilm reactor, packed bed bioreactor, trickling filter, etc.) were developed using either free cell or immobilized cell techniques to treat dye wastewater (Sonwani et al., 2021; Iqbal et al., 2022). Among these, moving bed biofilm reactors (MBBRs) are considered more promising for the bioremediation of azo dye wastewater. MBBR technology is based on the integration of a conventional activated sludge process (ASP) and attached biofilm system (Sonwani et al., 2021). MBBR system provides the advantage of both attached and suspended growth systems and minimizes the limitation of individual systems. The major advantages of the MBBR include stability against shock loading conditions, high biomass retention ability, less bio-clogging of the carrier, and higher removal efficiency (Castro et al., 2022; He et al., 2022). In addition, the biocarriers move in a random direction inside the bioreactor, which aids the better mass diffusion and high solid retention in the MBBR (Ong et al., 2020). Moreover, the biomass growth in the MBBR mainly depends upon the bio affinity and the surface characteristics

* Corresponding author.
E-mail address: rssingh.che@itbhu.ac.in (R.S. Singh).

https://doi.org/10.1016/j.biteb.2023.101375
Received 5 January 2023; Received in revised form 6 February 2023; Accepted 18 February 2023
Available online 24 February 2023

Nomenclature

Symbols and abbreviations

F_0	Initial dye concentration (mg/L)
F_t	Final dye concentration (mg/L)
Q	Volumetric feed flow rate (L/d)
V	Working volume of the bioreactor (L)
U_{max}	Maximum substrate removal rate (g/L. d)
K_B	Saturation constant (g/L. d)
r_{su}	Substrate utilization rate (g/L. d)
T	Hydraulic retention time (h)
X	Suspended biomass concentration (mg/L)
X_A	Attached biomass concentration (mg/L)
K_s	Half saturation constant (mg/L)
K	Specific substrate utilization rate (d^{-1})
Y	Biomass yield coefficient
k_d	Biomass decay rate (d^{-1})
PP	Polypropylene
$KMNO_4$-PP	$KMNO_4$ oxidised PP
$KMNO_4$-Ca-PP	$KMNO_4$ oxidised with Ca coated PP
EPS	Extracellular polymeric substance
SEPS	Soluble EPS
LB-EPS	Loosely-bound EPS
TB-EPS	Tightly-bound EPS
RSM	Response surface methodology
DOD	D-optimal design
MSK	modified Stover-Kincannon
RE	Removal efficiency

(hydrophilicity or hydrophobicity) of the biocarriers. Previously, various biocarriers, namely polypropylene (PP), polyethylene (PE), and high-density polyethylene (HDPE) have been utilized in MBBR for wastewater treatment due to their high stability and mechanical strength (Swain et al., 2022; Chen et al., 2020). However, most plastic biocarriers raise several demerits during the bioremediation of toxic pollutants, such as sluggishness in start-up due to slow biofilm growth and poor bacterial attachment (Mao et al., 2017).

Therefore, surface modification via chemical oxidation may be a useful technique to enhance the bacterial affinity of the hydrophobic carriers due to its being low-cost and easy to operation (Mahto and Das, 2022; Chen et al., 2012). According to Deng et al. (2016), chemical oxidation significantly improved the biomass growth on the peanut shell powder, and subsequently enhanced the bioremediation rate of pyrene. Recently, the calcium coating on the biocarrier has drawn significant attention. Coating the biocarrier surface with calcium compound reduces the hydrophobicity and enhances bacterial enzymatic activity (Ou et al., 2020). Gao et al. (2021) have investigated the bacterial affinity of a calcium-modified biocarrier to remove the nitrogenous compounds. They have reported that the bacterial adhesion ability and the secretion of extracellular polymeric substance (EPS) have been improved by 2.61 and 4.35 times, respectively, after adding calcium to the biocarrier surface. However, the literature review revealed that very few research works had been carried out on the chemical modification with calcium coating on the surface of polypropylene (PP) biocarrier.

The objective of the current work is to analyze the effect of the chemical modification on the bacterial affinity and surface properties of the PP biocarrier for effective biodegradation of azo dye. The conventional biocarrier (i.e., PP) and modified biocarriers (i.e., KMnO4-PP, KMnO4-Ca-PP) were filled in MBBR for the bioremediation of Acid blue 113 dye from wastewater. The process parameters (such as dye concentration and hydraulic retention time (HRT)) were optimized using response surface methodology (RSM) for maximum biodegradation Acid blue 113 dye from wastewater. Moreover, the substrate utilization rate and bacterial growth kinetics were studied using the modified Stover-Kincannon and Monod model, respectively.

2. Materials and methods

2.1. Chemicals and bacterial culture

The chemicals and other reagents used were of analytical grade. Acid blue 113 (AB 113) dye (C.I. no.: 26360, CAS no.: 3351-05-1) was purchased from Sigma Aldrich, India. The chemicals used to prepare minimal salt media (MSM), H_2SO_4, HCl, and $KMNO_4$ were procured from Merk, India. The composition of the MSM was followed (g/L): $MgSO_4$, 0.25; K_2HPO_4, 1.5; $FeCl_3$, 0.075; NH_4NO_3, 1.0; $CaCl_2$, 0.03; and $C_6H_{12}O_6$, 1.0. The synthetic textile wastewater was prepared by adding AB 113 dye in a suitable amount to the MSM and used for the bioremediation study. The pH of the synthetic wastewater was initially maintained at 6.5 ± 0.3.

The dye-contaminated soil sample was collected from a textile industry near Bhadohi, Uttar Pradesh, India, aseptically in a polypropylene bag to isolate potential microorganisms. The acclimatization of the microbes was carried out by adding 6.0 g of soil sample in a 100 mL MSM containing 25 mg/L of AB 113 dye. The solution was incubated in a rotary shaker (NSW Ltd., India) at 32 °C and 120 rpm for 10 days. Then, 15 mL of degraded sample was taken in a clean flask containing 50 mg/L of AB 113 dye. The incubation procedure was followed under similar environments. Finally, the adopted microorganisms were isolated using the serial dilution method followed by agar plates method. The isolated microbial species were stored at 4 °C for further application.

2.2. Identification of isolated bacterial species

The biochemical characterization and identification of isolated bacterial species were carried out at Triyat Scientific, Nagpur, India. 16S rRNA sequencing procedure was followed for bacterial identification. The EX pure Microbial DNA isolation kit developed by Bogar Bio Bee Shops Pvt. Ltd. was used to isolate the genomic DNA. India as per standard procedure (Swain et al., 2022). In the next stage, the polymerase chain reaction (PCR) method was followed to directly synthesize DNA from deoxy nucleotide substrates on a single-stranded DNA template using Taq DNA polymerase and universal primers. The PCR was operated under the following conditions; (i) initial denaturation at 95 °C for 2 min, (ii) denaturation at 95 °C for 30 s, (iii) annealing at 55 °C for 30 s, (iv) extension at 72 °C for 2 min, and (v) final extension at 72 °C for 10 min. Then, Single-pass sequencing was performed in an ABI 3730xl sequencer. The obtained nucleotide sequence was blast using NCBI blast similarity search tool (https://www.ncbi.nlm.nih.gov). Multiple sequence alignment was done after the phylogenetic analysis of the query sequence with the closely related sequence of the blast findings. The program MUSCLE 3.7 and Mega X software were used for the multiple alignments of sequences and construction of the phylogenetic tree, which is represented in Fig. 1. The isolated microbial species was identified as *Lysinibacillus macroides* KLM2 (accession number: MW599204) and *Lysinibacillus fusiformis* KLM1 (accession number: MW599200).

2.3. Development of modified biocarrier

The commercial polypropylene (PP, with a thickness of 1.3 cm and diameter of 2.5 cm) biocarriers were purchased from the Indiamart supplier. The specific surface area and density of the biocarrier were 520 m^2/m^3 and 920 kg/m^3, respectively. The PP biocarriers were stirred in a

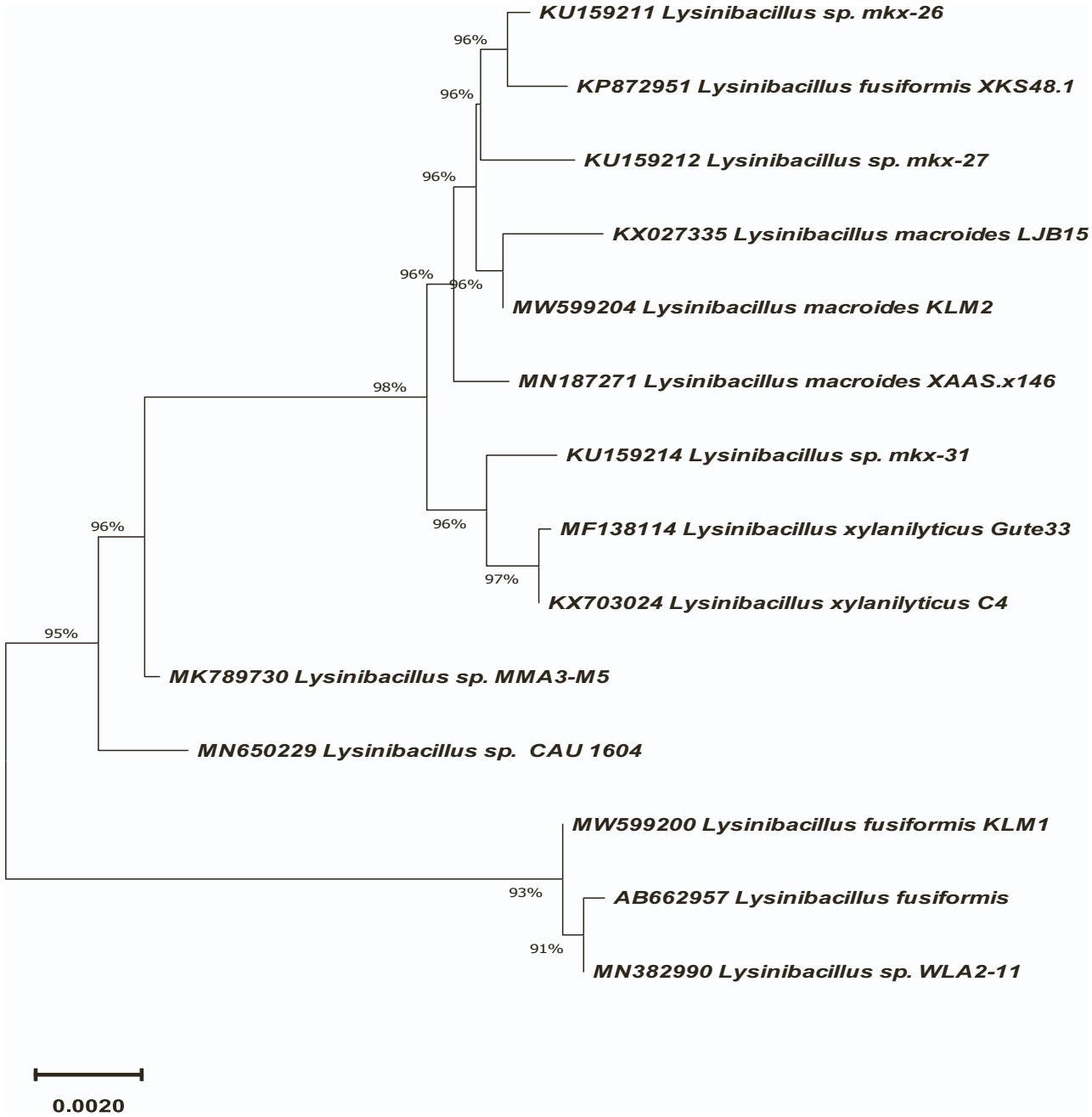

Fig. 1. Phylogenetic tree of the isolated bacterial species, i.e., *Lysinibacillus fusiformis* KLM1 (MW599200) and *Lysinibacillus macrolides* KLM2 (MW599204).

solution containing $KMNO_4$, distilled water, and H_2SO_4 in a ratio of 1:2:18 (m/m, %) at a temperature of 45 °C for 6.0 h. Then, the oxidised biocarriers were washed in a HCl solution (1.0 M) followed by washing in the phosphate buffer solution to remove the residual acid from the surface. The $KMNO_4$ treated PP biocarriers were immersed and stirred in $CaCl_2$ solution (2.0 M) at a temperature of 50 °C for 40 min. At the end, chemically modified biocarriers were dried at room temperature in the oven for use in bioremediation purposes. In the present study, a comparative analysis between three different biocarriers was used and abbreviated as PP (without modification), $KMON_4$-PP ($KMON_4$ oxidised PP), and $KMNO_4$-$CaCl_2$-PP (chemically oxidised with calcium coated PP) in the manuscript.

2.4. Quantification of attached biomass and extracellular polymeric substance on biocarriers

The effect of chemical oxidation and calcium coating on the amount of biomass growth was investigated in batch studies. Each type of PP biocarriers was filled in moving bed biofilm reactors (MBBRs), which were operated for 15 days. The MBBRs were fed with synthetic wastewater along with AB 113 dye of 50 mg/L concentration. During the batch study, the dissolved oxygen concentration was maintained at 6.0 ± 1.0 mg/L. The volatile attached solids (VAS) were evaluated using the gravimetric method after 20 days of operation (APHA, AWWA, WEF, 2005).

Moreover, the extracellular polymeric substance (EPS) was measured according to the standard procedure (Gao et al., 2021). In brief, the immobilized biocarriers were transferred to a beaker containing 100 mL of distilled water and then sonicated in an ultra sonicator

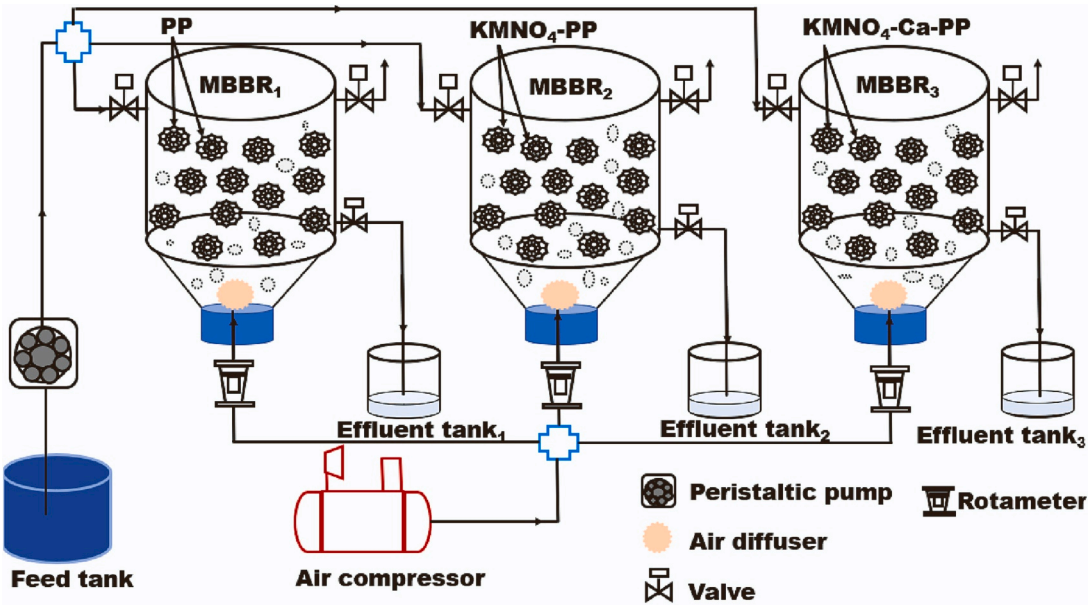

Fig. 2. A schematic diagram of MBBRs used for AB 113 dye bioremediation.

(Labman Scientific Instruments, India) at a temperature of 4 °C for 1.0 min. The suspended solid was settled using a refrigerated centrifuge machine (REMI, RM - 12C BL) at 4000 rpm for 10 min. The supernatant liquid was extracted and filtered to obtain soluble EPS (SEPS). In the second stage, the sediment obtained in the previous step was added to 100 mL of distilled water and incubated for 1.0 h. Then the solution was centrifuged and the supernatant liquid was filtered through a 0.45 μm membrane to obtain loosely-bound EPS (LB-EPS). The remaining solid was resuspended in 100 mL distilled water and again incubated at 80 °C for 40 min. Again, the solution was centrifuged (8000 rpm for 10 min) and filtered through a membrane to measure tightly-bound EPS (TB-EPS).

2.5. Moving bed biofilm reactors set-up and operational procedure

Three cylindrical bioreactors, made up of borosilicate glass, were fabricated (internal diameter of 12 cm and height of 22 cm). The total capacity and working volume of the bioreactors were 1.8 and 1.5 L, respectively. Each bioreactor was associated with a feed tank, effluent tank, air compressor, and rotameter, as shown in Fig. 2. The stone diffusers that were affixed to the tank's bottom were used to distribute the air. The filling ratio of the PP biocarriers in MBBR was kept at 45 % (*v*/*v*). As discussed in Section 2.1, the isolated bacterial culture was used as inoculum in MBBR to degrade the AB 113 dye from wastewater.

The bioreactors were operated in a batch mode to immobilize the bacterial species on the surface of biocarriers. The synthetic wastewater containing AB 113 dye (50 mg/L) and the bacterial inoculum was fed to the MBBRs for 15 days. After 15 days of batch operation, the MBBRs were switched to continuous mode and run according to the designed experiments set by the response surface methodology. The pH of the wastewater and dissolved oxygen was maintained at 7.0 ± 1.0 and 6.0 ± 1.0 mg/L, respectively.

2.6. Optimization of process variables using response surface methodology

The experimental design was formulated using the D-optimal design (DOD) of response surface methodology (RSM). The mathematical and statistical tool is effective in terms of cost-saving and less time-consuming while designing the bioreactor system (Zinatizadeh and Ghaytooli, 2015). In this study, two independent process variables, such as AB 113 dye concentration (50–150 mg/L) and hydraulic retention time (HRT) (16–48 h) along with types of biocarriers (PP, $KMNO_4$-PP, $KMNO_4$-Ca-PP) as a categorical factor were chosen for the optimization. Based on the process ranges, the Design-Expert software (Version 13) generated a series of experiments at the specific conditions summarized in Table.1. Total 39 number of experiments, including 15 central points

Table 1
Experimental conditions obtained from RSM study and the corresponding responses.

Run	Factor 1 *A*: HRT (h)	Factor 2 *B*: dye concentration (mg/L)	Factor 3 *C*: types of biocarrier	Response dye removal efficiency (%)
1	16	50	$KMNO_4$-Ca-PP	42.03 ± 2.79
2	48	150	$KMNO_4$-Ca-PP	72.25 ± 3.01
3	48	100	PP	62.36 ± 1.66
4	16	150	$KMNO_4$-Ca-PP	24.42 ± 1.03
5	32	100	$KMNO_4$-Ca-PP	68.67 ± 2.40
6	16	150	PP	19.6 ± 3.26
7	48	150	$KMNO_4$-Ca-PP	72.25 ± 2.73
8	16	150	$KMNO_4$-Ca-PP	26.04 ± 1.96
9	16	50	$KMNO_4$-PP	37.17 ± 3.41
10	48	50	$KMNO_4$-Ca-PP	88.57 ± 3.78
11	48	150	$KMNO_4$-PP	67.12 ± 2.94
12	16	50	$KMNO_4$-Ca-PP	40.79 ± 1.06
13	48	50	PP	67.94 ± 1.59
14	32	150	$KMNO_4$-PP	53.08 ± 3.21
15	16	100	$KMNO_4$-PP	33.61 ± 1.44
16	48	50	$KMNO_4$-Ca-PP	90.27 ± 1.35
17	16	50	$KMNO_4$-Ca-PP	40.57 ± 3.27
18	16	50	$KMNO_4$-PP	37.17 ± 2.51
19	16	50	PP	28.34 ± 2.97
20	32	50	$KMNO_4$-PP	69.2 ± 3.05
21	32	100	PP	45.73 ± 2.28
22	16	150	PP	20.49 ± 1.16
23	32	150	PP	40.98 ± 3.40
24	48	100	$KMNO_4$-PP	71.48 ± 3.56
25	16	150	$KMNO_4$-PP	25.13 ± 2.79
26	16	100	PP	23.04 ± 1.38
27	48	50	$KMNO_4$-PP	80.23 ± 1.62
28	48	150	$KMNO_4$-PP	65.82 ± 2.90
29	48	50	PP	68.3 ± 1.74
30	48	150	PP	55.29 ± 2.35

RSM: Response surface methodology; HRT: Hydraulic retention time; PP: Polypropylene; $KMNO_4$-PP: $KMNO_4$ oxidised PP; $KMNO_4$-Ca-PP: $KMNO_4$ oxidised with Ca coated PP.

Table 2
ANOVA analysis of the quadratic model.

Response: dye removal efficiency					
Source	Sum of squares	*Df*	Mean square	*F* value	*p*-Value
Model	13,237.23	11	1203.39	311.36	<0.0001
A - HRT	10,859.83	1	10,859.83	2809.78	<0.0001
B - dye concentration	1110.73	1	1110.73	287.38	<0.0001
C - biocarrier	1110.33	2	553.67	143.25	<0.0001
AB	10.39	1	10.39	2.69	0.1184
AC	102.92	2	51.46	13.31	0.0003
BC	25.26	2	12.63	3.27	0.0615
A^2	195.26	1	195.26	50.52	<0.0001
B^2	0.2258	1	0.2258	0.0584	0.8118
Residual	69.57	18	3.87		
Lack of fit	64.27	9	7.14	12.12	0.0005
Pure error	5.30	9	0.5891		
Cor total	13,306.90	29			

ANOVA: Analysis of variance; HRT: Hydraulic retention time.

and 24 non-central points, were designed in this study.

The process responses (dye removal efficiency) were measured during the experiments and used to evaluate the coefficients of a quadratic expression (Eq. (1)).

$$A = \alpha + \alpha_i\, Y_i + \alpha_j\, Y_j + \alpha_{ij}\, Y_{ij} + \alpha_{ii}\, Y_i^2 + \alpha_{jj}\, Y_j^2 + \quad (1)$$

where A is the dye removal efficiency (%) and α denotes the correlation coefficients. In addition, i and j represent the coefficients of multi-degree. ANOVA analysis was also performed to determine the model's significance, and the results are detailed in Table 2. The quadratic model's applicability to the collected data is shown by a greater F-value and a lower p-value (<0.05).

2.7. Analytical methods

The morphology of the plastic biocarrier was studied using scanning electron microscopy (SEM, QUANTA 200F, Netherland) technique. The surface elemental composition of the modified biocarriers was analysed using X-ray photoelectron spectroscopy (XPS, K-Alpha, Thermo Fisher Scientific, India). The hydrophobicity of the biocarriers was determined using a contact angle (KRUSS, Germany) instrument. In addition, the bioremediation was monitored by analysing the functional group using Nicolet iS5 FTIR spectrophotometer. Moreover, the liquid samples were centrifuged at 5500 rpm for 12 min. The concentration of AB 113 dye was measured using a UV–Vis spectrophotometer (ELICO, SL-210, India). The removal efficiency (RE) of AB 113 dye was measured using the following expression as

$$\text{RE}\ (\%) = \frac{F_0 - F_t}{F_0} \times 100 \quad (2)$$

where F_0 and F_t are the initial and final dye concentrations (mg/L), respectively.

2.8. Kinetic analysis

Kinetic modeling is a suitable approach to design and control the outcomes in bioremediation study by developing mathematical correlations between the process variables and the responses (Nga et al., 2020). The present study used two kinetic models, namely modified Stover-Kincannon (MSK) and Monod models. The MSK model predicts the behaviour of the attached growth bioreactors by estimating the substrate consumption rate at various organic loading rates. In addition, the desired capacity of the bioreactor to attain a specific pollutant concentration can be estimated using the MSK model (Sonwani et al., 2021). The Monod model is preferred to describe the growth kinetics behaviour of the microbial species in a continuous bioreactor (Shahzad et al., 2022).

2.8.1. Modified Stover-Kincannon model

Initially, the Stover-Kincannon model was developed to correlate the substrate utilization rate with the organic loading rate in a rotating biological contactor. However, the model was later simplified by replacing the surface area of the active biomass with the total volume of the bioreactor (Faridnasr et al., 2016). The modified model can be expressed as follows:

$$\frac{dF_t}{dt} = \frac{Q}{V}\,(F_0 - F_t) = \frac{U_{max}\left(\frac{Q.F_0}{V}\right)}{K_B + \left(\frac{Q.F_0}{V}\right)} \quad (3)$$

where Q, V, U_{max}, and K_B represent the volumetric feed flow rate (L/d), operational volume of the bioreactor (L), maximum substrate removal rate (g/L. d), and saturation constant (g/L. d), respectively.

Now, a straight-line equation can be formed by rearranging the Eq. (3) as

$$\frac{1}{\frac{dF_t}{dt}} = \frac{V}{Q.(F_0 - F_t)} = \frac{K_B.V}{U_{max.Q.F_0}} + \frac{1}{U_{max}} \quad (4)$$

The value of U_{max}, and K_B can be obtained from the slope and intercept of the graph plotted between $\frac{V}{Q.(F_0 - F_t)}$ and $\frac{V}{Q.F_0}$.

2.8.2. Monod model

Assuming the MBBR acts as a continuous stirred tank reactor, the mass balance of the substrate can be written as.

$$V.\frac{dF_t}{dt} = Q.F_0 – Q.F_t + V.rsu \quad (5)$$

where r_{su} is the substrate utilization rate (g/L. d).

At steady state-condition, the value of $\frac{dF_t}{dt}$ will be negligible. Therefore, Eq. (5) can be reduced to the obtain the final expression for r_{su} as follows:

$$rsu = -\frac{F_0 - F_t}{t} \quad (6)$$

According to the Monod model, r_{su} can be written in the form of Eq. (7) as

$$rsu = -\frac{k.F_t.X}{K_s + F_t} \quad (7)$$

Now, by equalizing and rearranging the right-hand side of the Eqs. (6) and (7), the final expression can be written as Eq. (8):

$$\frac{t.X}{(F_0 - F_t)} = \frac{K_s}{k} \times \frac{1}{F_t} + \frac{1}{k} \quad (8)$$

where t and X denote the hydraulic retention time (h) and biomass concentration in the bioreactor (g *V*SS/L). In addition, K_s and k are the half-saturation constant (mg/L) and specific substrate utilization rate (d^{-1}), respectively.

Similarly, the biomass balance inside the bioreactor can be written as follows.

$$V.\frac{dX}{dt} = Q.X_0 – Q.X + V.rg \quad (9)$$

$$rg = \frac{\mu_{max.X.S}}{K_s + S} kd.X \quad (10)$$

At steady-state conditions, the final equation for the bacterial mass balance can be obtained by integrating and rearranging the Eqs. (9) and (10) as

$$\frac{F_0 - F_t}{X} = \frac{k_d}{Y} \times \frac{t.X_A}{X} + \frac{1}{Y} \quad (11)$$

Table 3
Summary of contact angles, attached biomass, and extracellular polymeric substance associated with various biocarriers.

Types of biocarriers	Contact angle (°)	Attached biomass (mg/L)	EPS (mg/g VSS)	SEPS (mg/g VSS)	LB-EPS (mg/g VSS)	TB-EPS (mg/g VSS)
PP	94 ± 3.28	450 ± 8.93	12.5	4.01	1.03	7.46
$KMNO_4$-PP	79 ± 2.74	590 ± 10.57	21.98	6.73	2.36	12.89
$KMNO_4$-Ca-PP	70 ± 2.95	680 ± 8.50	26.7	8.49	3.02	15.19

EPS: extracellular polymeric substance; SEPS: Soluble EPS; LB-EPS: Loosely-bound EPS; TB-EPS: Tightly-bound EPS; VSS: Volatile suspended solid.

where X, X_A, Y, and k_d are the suspended biomass (g VSS/L), attached biomass (g VSS/L), biomass yield coefficient, and biomass decay rate (d^{-1}), respectively. The value of Y and k_d can be evaluated from the slope and intercept of the graph plotted between $\frac{F_0-F_t}{X}$ and $\frac{t.X_A}{X}$.

3. Results and discussions

3.1. Surface morphology and chemical composition of the biocarrier

The SEM images representing the PP biocarrier exhibit a smooth and a flat surface (Supplementary material). The biocarrier was found to be hydrophobic, having a contact angle of 94° (Table 3). However, the chemical oxidation and calcium deposition on the biocarrier provided a hydrophilic and wrinkled surface for high biomass growth. The contact angle of the $KMNO_4$-PP and $KMNO_4$-Ca-PP biocarriers were measured to be 79° and 70°, respectively. The bacterial affinity was found to be increased on a hydrophilic and rough surface due to the increase of the

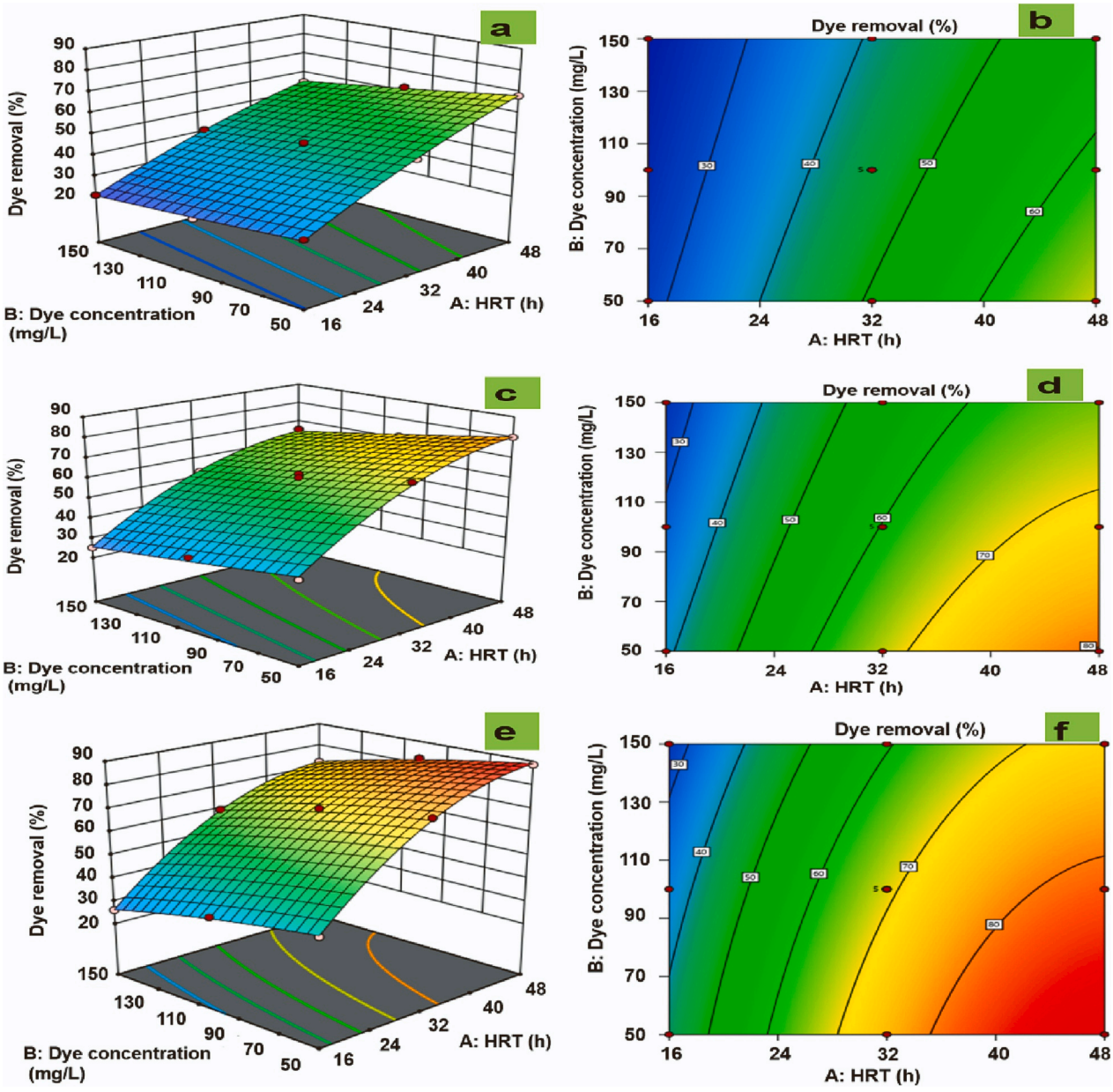

Fig. 3. The interactive effect of initial dye concentration and HRT on dye removal efficiency (%) in MBBRs filled with (a, b) PP; (c, d) $KMNO_4$–PP; (e, f) $KMNO_4$–Ca–PP biocarriers.

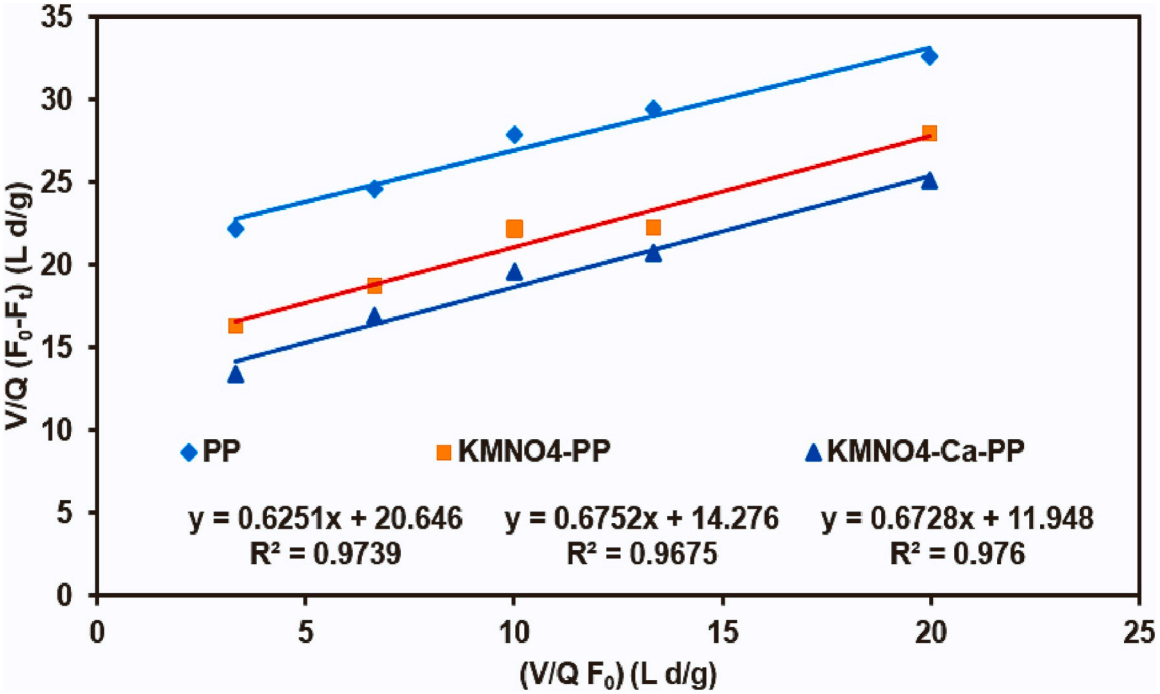

Fig. 4. Modified Stover-Kincannon kinetic model used in bioremediation of AB 113 dye in MBBRs for PP, $KMNO_4$–PP, and $KMNO_4$ –Ca–PP biocarriers.

secretion of proteins, nucleic acid, and extracellular polymeric substances (Gao et al., 2021).

The elemental composition of the biocarriers (before and after modification) was studied using XPS analysis (Supplementary material). The PP (raw) was mainly composed of C (98.84 %) and O (1.16 %). However, Mn and Ca peaks were introduced after surface modification with $KMNO_4$ and $CaCl_2$. K and Mn peaks appeared at 292.6 and 642.53 eV, respectively. Similarly, two strong peaks, i.e., Ca_2p and Cl_2p spectrum, revealed the successful deposition of the Ca element in the form of $CaCl_2$ on the surface of the PP biocarrier.

3.2. Effect on immobilized biomass growth and extracellular polymeric substance secretion

The evaluation of biomass growth was carried out in the batch MBBR using three different types of biocarriers and the attached biomass was quantified after 15 days of operation. The biomass growth mainly depends upon the secretion of the extracellular polymeric substance (EPS) by bacteria. The attached biomass of 450 mg/L was measured with the PP biocarrier (Table 3). However, the amount of volatile suspended solid was improved with chemical oxidation and calcium treatment. Moreover, the quantity of biomass was increased by 31.11 and 51.11 % after $KMNO_4$ oxidation and $CaCl_2$ treatment. Similarly, the EPS secretion was also improved with the chemical treatment of the plastic surface. The EPS was increased by 75.84 % and 113.6 % when the PP (raw) biocarriers were treated with $KMNO_4$ and $CaCl_2$, respectively. The significant improvement in attached growth biomass and EPS was due to the hydrophilicity, which enhances the binding of bio cells on the biocarrier surface. The attachment of calcium element acts as a micronutrient for the bacterial cells.

3.3. Statistical analysis

D-optimal design is an effective Response surface methodology (RSM) technique that enables the prediction of an accurate response with a smaller number of experiments (Bahadi et al., 2019). The experimental conditions were designed based on the range of independent process variables and a total of 30 experiments were performed. The responses (i.e., dye removal efficiency (RE)) were evaluated at each condition and summarized in Table 1. The statistical significance of the obtained quadratic model was investigated by using ANOVA analysis. The low value of p (<0.0001) represented the model predictability to estimate the process response. In addition, the regression coefficients were evaluated to evaluate the fit of the model and found to be 0.995, 0.992, and 0.986 for R^2, adjusted R^2, and predicted R^2, respectively.

3.4. The effect of the process variables on dye removal efficiency

The effect of HRT and initial dye concentration was studied in the MBBRs. The corresponding dye removal efficiency (RE) was measured and provided in Table 1. The present study showed that the removal of azo dye was significantly affected by the change of HRT and initial dye concentration. The RE was observed to be enhanced with a change in HRT for each type of biocarrier (Fig. 3). The RE was increased from 23.04 to 45.73 % with an increase in HRT varied from 16 to 32 h (dye concentration = 100 mg/L; biocarrier type = PP) (Table 1). With a further increase of HRT, the RE attained a maximum value of 62.36 % at similar operating conditions. The bioremediation process needs sufficient time for the substrate and microorganisms to interact completely. The washout of the pollutants without reaching the surface of the active bacterial site resulted in low RE (Banerjee and Ghoshal, 2016). However, the initial dye concentration was observed to be followed an inverse relation with the RE. At an initial dye concentration of 150 mg/L, the lowest RE of 67.12 % was found (HRT = 48 h; biocarrier type = $KMNO_4$-PP). The RE was drastically improved when the dye concentration was reduced to 50 mg/L and measured to be 80.23 % at similar conditions. The significant drop of RE at a higher concentration was due to the change in the organic loading rate, which decreased the performance of MBBR.

The efficacy of the MBBR was greatly affected by the types of biocarrier. The maximum dye RE of 90.27 and 80.23 % was obtained by the MBBR filled with $KMNO_4$-Ca-PP and $KMNO_4$-PP biocarriers, respectively (HRT of 48 h and dye concentration of 50 mg/L). In the meantime, the MBBR filled with and PP biocarriers could attain a RE of 68.3 %. The better performance shown by $KMNO_4$-Ca-PP biocarriers was due to the hydrophilic surface, which stimulates the high biomass attachment

Table 4
Various kinetic parameters obtained from modified Stover-Kincannon and Monod model.

Model name	Coefficients	Types of biocarrier		
		PP	$KMNO_4$-PP	$KMNO_4$-Ca-PP
Modified Stover-Kincannon	U_{max} (g/L. d)	0.048	0.070	0.083
	K_B (g/L. d)	0.030	0.047	0.056
	R^2	0.974	0.967	0.976
	RMSE	0.586	0.708	0.603
Monod	k (d^{-1})	0.387	0.926	1.896
	K_s (mg/L)	116. 99	400.89	1158.47
	R^2	0.960	0.958	0.935
	RMSE	0.786	0.723	0.788
	Y	17.006	19.417	28.818
	K_d (mg/L)	0.167	0.212	0.386
	R^2	0.909	0.950	0.966
	RMSE	1.001	0.909	0.915

PP: Polypropylene; $KMNO_4$-PP: $KMNO_4$ oxidised PP; $KMNO_4$-Ca-PP: $KMNO_4$ oxidised with Ca coated PP; RMSE: Root mean square error.

within a specific time period. In addition, the Calcium deposition on the plastic surface promoted the production of EPS which enhanced the metabolic activity of the bacterial cells. Therefore, the chemically modified biocarrier (i.e., $KMNO_4$-Ca-PP) could be more effective for treating azo dye wastewater than the traditional PP biocarrier.

3.5. Verification of the model through numerical optimization

The precision of the designed model was investigated at a maximum HRT (48 h), a suitable initial dye concentration (100 mg/L), and the effective biocarrier ($KMNO_4$-Ca-PP) for maximum dye RE. The predicted value of the dye RE was 81.54 %, with desirability of 0.936. Further, real-time experiments were conducted at the above process conditions and the RE was evaluated to be 83.75, 73.52, and 61.24 % for $KMNO_4$-Ca-PP, $KMNO_4$-PP, and PP biocarriers, respectively. The minimal error (within 3.0 %) between the predicted and experimental values represented the reasonable accuracy of the model.

3.6. Kinetic evaluation

3.6.1. Modified Stover-Kincannon model

The values of maximum substrate utilization rates (U_{max}) and saturation constants (K_B) were calculated from the slopes and intercepts obtained from Fig. 4. The high values of regression coefficients ($R^2 > 0.96$) represented the significant fitness of the kinetic model to predict the parameters. In addition, the kinetic analysis showed that the dye utilization rates were significantly increased with surface modification of the biocarrier and evaluated to be 0.048, 0.070, and 0.083 g/L. d for PP, $KMNO_4$-PP, and $KMNO_4$-Ca-PP, respectively (Table 4). Similarly, the corresponding rate constants (K_B) were calculated to be 0.03, 0.047, and 0.056, respectively.

3.6.2. Monod model

The dependency of the dye degradation rate on the microbial growth in the MBBR was studied by plotting a graph between $\frac{t.X}{(F_0-F_t)}$ and $\frac{1}{F_t}$ (Fig. 5a). The values of specific substrate utilization rate (k) and half-saturation constant (K_s) were calculated for each type of biocarrier and summarized in Table 4. It was obvious that better k values were observed for MBBR filled with $KMNO_4$-Ca-PP biocarriers with regression coefficients of 0.96. Moreover, the deducted values of \k were to be 1.896, 0.926, and 0.387 d^{-1} for PP, $KMNO_4$-PP, and $KMNO_4$-Ca-PP biocarriers, respectively. Similarly, Y and k_d values were calculated from the graph plotted against $\frac{F_0-F_t}{X}$ vs. $\frac{t.X_A}{X}$ (Fig. 5b). It can be seen that the model has provided a satisfactory result with significant regression coefficients ($R^2 > 0.90$) for each type of biocarrier. The biomass yield coefficients (Y) were improved with surface modification and found to be 17.006, 19.417, and 28.818 for PP, $KMNO_4$-PP, and $KMNO_4$-Ca-PP biocarriers, respectively. In the meantime, the corresponding biomass decay rates (k_d) were measured and resulted to be 0.167, 0.212, 0.386 mg/L, respectively.

3.7. FTIR analysis

After the bioremediation process, the FTIR analysis was employed to analyze the broad change of functional groups in the AB 113 dye. A comparative FTIR spectrum of untreated and treated wastewater was depicted in the Supplementary material. The analysis showed that the

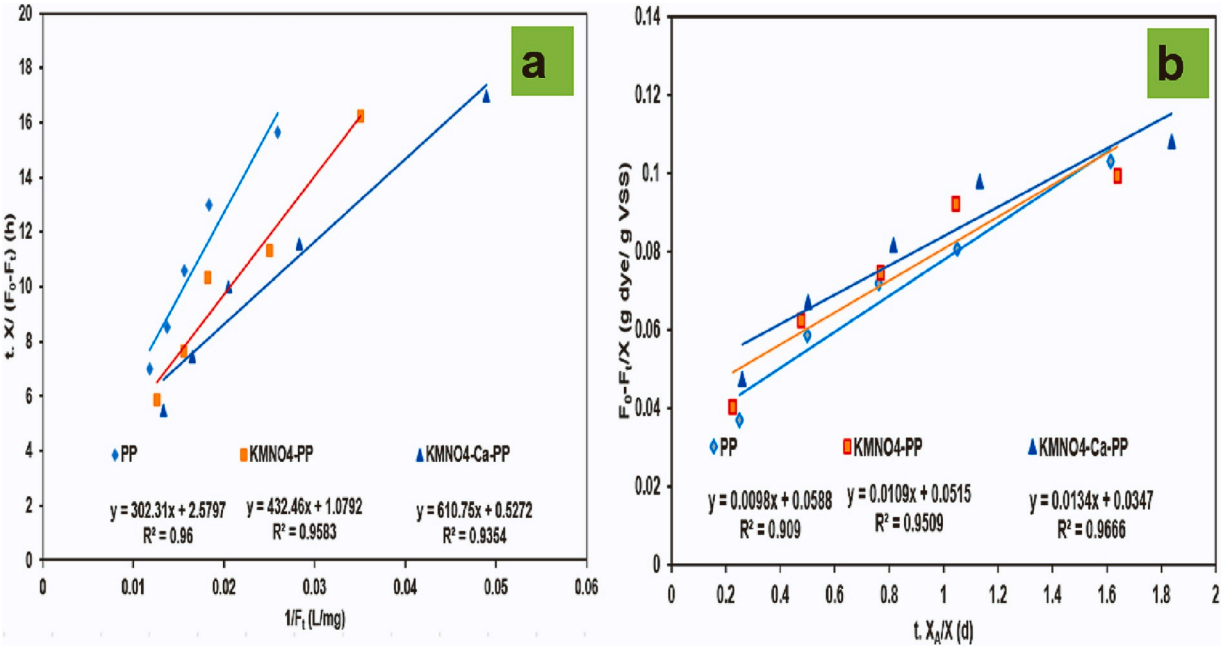

Fig. 5. Monod model used in bioremediation of AB 113 dye in MBBRs for PP, $KMNO_4$–PP, and $KMNO_4$–Ca–PP biocarriers.

azo bond (N═N), mainly identified at a bandgap between 1504 and 1555 cm^{-1}, is absent in the degraded sample. Comparatively broad and strong intensities of spectra were detected at 3300–3500 cm^{-1} in the treated sample, revealing the formation of hydroxyl (OH) and amino (NH) groups in bioremediation. In addition, the appearance of peaks at 1635 cm^{-1} and 1635 cm^{-1} correspond to the presence of N—H bonding and C (NH)═O group, respectively. The significant shift of the peaks was observed at wavenumbers of 1066 cm^{-1}. Moreover, the spectrum at 1397 cm^{-1} corresponds to the C—H bending, 1635 cm^{-1} refers to N—H bending vibration, and 1066 cm^{-1} denotes the stretching vibration of C—O groups. The present functional group analysis indicated the degradation of Acid Blue 113 dye.

4. Conclusion

A polymeric biocarrier (i.e., PP) was modified to biodegrade the AB 113 dye from wastewater effectively. The chemical oxidation and calcium treatment of the biocarrier enhance the start-up time period and biomass attachment. The batch investigation found that the modified biocarrier enhanced the fixed biomass and extracellular polymeric material secretion by 1.51 and 2.13 times, respectively. Moreover, at optimized process conditions, KMNO4-Ca-PP biocarriers showed a maximum dye RE of 83.75 % due to the more fixed biofilm development. Therefore, the modified biocarrier in MBBR can be effectively employed to treat the azo dyes from wastewater.

CRediT authorship contribution statement

The contribution of all authors is given below:

Kanhaiya Lal Maurya: Software, Conceptualization, Methodology, Writing-original draft,

Mohit Kumar: Writing, Data calculation.

Ravi Kumar Sonwani: Review, Software.

Vivek Jaiswal: Formal investigation, Review, and Editing of original draft.

Ankur Verma: Supervision, Validation.

Ram Sharan Singh*: Supervision, Review, Validation.

Declaration of competing interest

I declare that this is an original research work of the authors and all the authors have contributed in completion of this work, which is embedded in this paper.I also confirm that this work has not been published elsewhere nor it is currently under consideration for publication elsewhere. I have no conflict of interest.

Data availability

Data will be made available on request.

Acknowledgments

The author (Kanhaiya Lal Maurya) gratefully acknowledged the Ministry of Education (India) for granting financial support and the Indian Institute of Technology, BHU, Varanasi, India, for providing a laboratory facility to carry out the research work. The authors are also acknowledging the Vikram Sarabhai Space Center, ISRO (R&D/SA/ISRO/CHEM/19-20/06) for providing funds to create infrastructure which was used for the present study.

Appendix A. Supplementary data

Supplementary data to this article can be found online at https://doi.org/10.1016/j.biteb.2023.101375.

References

1 American Public Health Association, American Water Works Association, Water Environment Federation, 2005. Standard Methods for the Examination of Water and Wastewater, 21th ed. Washington, DC.
2 Bahadi, M., Yusoff, M.F., Salimon, J., Derawi, D., 2019. Optimization of response surface methodology by D-optimal design for synthesis of food-grade palm kernel based biolubricant. Ind. Crop. Prod. 139, 111452 https://doi.org/10.1016/j.indcrop.2019.06.015.
3 Banerjee, A., Ghoshal, A.K., 2016. Biodegradation of phenol by calcium-alginate immobilized@@ Bacillus cereus in a packed bed reactor and determination of the mass transfer correlation. J. Environ. Chem. Eng. 4 (2), 1523–1529. https://doi.org/10.1016/j.jece.2016.02.012.
4 Barathi, S., Karthik, C., Nadanasabapathi, S., Padikasan, I.A., 2020. Biodegradation of textile dye reactive blue 160 by Bacillus firmus (Bacillaceae: Bacillales) and non-target toxicity screening of their degraded products. Toxicol. Rep. 7, 16–22. https://doi.org/10.1016/j.toxrep.2019.11.017.
5 Castro, F.D., Lemos, F.R., Bassin, J.P., 2022. Removal of Dyes from Wastewaters in Moving Bed Biofilm Reactors: A Review of Biodegradation Pathways and Treatment Performance. In: Muthu, S.S., Khadir, A. (Eds.), Dye Biodegradation, Mechanisms and Techniques. Sustainable Textiles: Production, Processing, Manufacturing & Chemistry. Springer, Singapore, pp. 227–262. https://doi.org/10.1007/978-981-16-5932-4_9.
6 Chen, S., Cheng, X., Zhang, X., Sun, D., 2012. Influence of surface modification of polyethylene biocarriers on biofilm properties and wastewater treatment efficiency in moving-bed biofilm reactors. Water Sci. Technol. 65 (6), 1021–1026. https://doi.org/10.2166/wst.2012.915.
7 Chen, Y.T., Xie, X.L., Zou, S.Q., Qiu, R., Zhong, G.J., Lai, B., Li, Z.M., 2020. Tailored surface porosity of polyethylene-based co-continuous structures for moving bed biofilm reactor carriers. ACS Appl. Polym. Mater. 2 (8), 3226–3233. https://doi.org/10.1021/acsapm.0c0038.
8 Deng, F., Liao, C., Yang, C., Guo, C., Dang, Z., 2016. Enhanced biodegradation of pyrene by immobilized bacteria on modified biomass materials. Int. Biodeterior. Biodegrad. 110, 46–52. https://doi.org/10.1016/j.ibiod.2016.02.016.
9 Emadi, Z., Sadeghi, M., Forouzandeh, S., Sadeghi, R., Mohammadi-Moghadam, F., 2022. Simultaneous decolorization/degradation of AB-113 and chromium (VI) removal by a salt-tolerant Klebsiella sp. AB-PR and detoxification of biotransformed-metabolites. IntJ. Environ. Sci. Technol. 19 (3), 2007–2024. https://doi.org/10.1007/s13762-021-03360-9.
10 Faridnasr, M., Ghanbari, B., Sassani, A., 2016. Optimization of the moving-bed biofilm sequencing batch reactor (MBSBR) to control aeration time by kinetic computational modeling: simulated sugar-industry wastewater treatment. Bioresour. Technol. 208, 149–160. https://doi.org/10.1016/j.biortech.2016.02.047.
11 Gao, F., Zhou, X., Ma, Y., Zhang, X., Rong, X., Xiao, X., Wu, Z., Wei, J., 2021. Calcium modified basalt fiber bio-carrier for wastewater treatment: Investigation on bacterial community and nitrogen removal enhancement of bio-nest. Bioresour. Technol. 335, 125259 https://doi.org/10.1016/j.biortech.2021.125259.
12 Giri, B.S., Goswami, M., Kumar, P., Yadav, R., Sharma, N., Sonwani, R.K., Singh, R.S., 2020. Adsorption of patent blue V from textile industry wastewater using sterculia alata fruit shell biochar: evaluation of efficiency and mechanisms. Water 12 (7), 2017. https://doi.org/10.3390/w12072017.
13 He, S., Song, N., Yao, Z., Jiang, H., 2022. An assessment of the purification performance and resilience of sponge-based aerobic biofilm reactors for treating polluted urban surface waters. Environ. Sci. Pollut. Res. 1–14 https://doi.org/10.1007/s11356-022-19083-4.
14 Iqbal, A., Ali, N., Shang, Z.H., Malik, N.H., Rehman, M.M.U., Sajjad, W., Rehman, M. L.U., Khan, S., 2022. Decolorization and toxicity evaluation of simulated textile effluent via natural microbial consortia in attached growth reactors. Environ. Technol. Innov. 102284 https://doi.org/10.1016/j.eti.2022.102284.
15 Joshi, A.U., Hinsu, A.T., Kotadiya, R.J., Rank, J.K., Andharia, K.N., Kothari, R.K., 2020. Decolorization and biodegradation of textile di-azo dye Acid Blue 113 by Pseudomonas stutzeri AK6. 3 Biotech 10 (5), 1–16. https://doi.org/10.1007/s13205-020-02205-5.
16 Kapoor, R.T., Danish, M., Singh, R.S., Rafatullah, M., HPS, A.K., 2021. Exploiting microbial biomass in treating azo dyes contaminated wastewater: Mechanism of degradation and factors affecting microbial efficiency. J Water Process Eng 43, 102255. https://doi.org/10.1016/j.jwpe.2021.102255.
17 Khan, M.D., Li, D., Tabraiz, S., Shamurad, B., Scott, K., Khan, M.Z., Yu, E.H., 2021. Integrated air cathode microbial fuel cell-aerobic bioreactor set-up for enhanced bioelectrodegradation of azo dye Acid Blue 29. Sci. Total Environ. 756, 143752 https://doi.org/10.1016/j.scitotenv.2020.143752.
18 Mahto, K.U., Das, S., 2022. Bacterial biofilm and extracellular polymeric substances in the moving bed biofilm reactor for wastewater treatment: a review. Bioresour. Technol. 345, 126476 https://doi.org/10.1016/j.biortech.2021.126476.
19 Mao, Y., Quan, X., Zhao, H., Zhang, Y., Chen, S., Liu, T., Quan, W., 2017. Accelerated startup of moving bed biofilm process with novel electrophilic suspended biofilm carriers. Chem. Eng. J. 315, 364–372. https://doi.org/10.1016/j.cej.2017.01.041.
20 Maurya, K.L., Swain, G., Sonwani, R.K., Verma, A., Singh, R.S., 2022. Biodegradation of Congo red dye using polyurethane foam-based biocarrier combined with activated carbon and sodium alginate: batch and continuous study. Bioresour. Technol. 126999 https://doi.org/10.1016/j.biortech.2022.126999.
21 Mishra, S., Maiti, A., 2018. The efficacy of bacterial species to decolourise reactive azo, anthroquinone and triphenylmethane dyes from wastewater: a review. Environ. Sci. Pollut. Res. 25 (9), 8286–8314. https://doi.org/10.1007/s11356-018-1273-2.

22 Nga, D.T., Hiep, N.T., Hung, N.T.Q., 2020. Kinetic modeling of organic and nitrogen removal from domestic wastewater in a down-flow hanging sponge bioreactor. Environ. Eng. Res. 25 (2), 243–250. https://doi.org/10.4491/eer.2018.390.
23 Ong, C., Lee, K., Chang, Y., 2020. Biodegradation of mono azo dye-reactive orange 16 by acclimatizing biomass systems under an integrated anoxic-aerobic REACT sequencing batch moving bed biofilm reactor. J. Water Process. Eng. 36, 101268 https://doi.org/10.1016/j.jwpe.2020.101268.
24 Ou, Q., Xu, Y., Li, X., He, Q., Liu, C., Zhou, X., Wu, Z., Huang, R., Song, J., Huangfu, X., 2020. Interactions between activated sludge extracellular polymeric substances and model carrier surfaces in WWTPs: a combination of QCM-DAFM and XDLVO prediction. Chemosphere 253, 126720. https://doi.org/10.1016/j.chemosphere.2020.126720.
25 Rosu, C.M., Avadanei, M., Gherghel, D., Mihasan, M., Mihai, C., Trifan, A., Vochita, G., 2018. Biodegradation and detoxification efficiency of azo-dye reactive orange 16 by pichia kudriavzevii CR-Y103. Wat Air Soil Pollut. 229 (1), 118. https://doi.org/10.1007/s11270-017-3668.
26 Shahzad, H.M.A., Khan, S.J., Habib, Z., 2022. Performance evaluation and substrate removal kinetics in a thermophilic anaerobic moving bed biofilm reactor for starch degradation. Water Pract. Technol. 17 (1), 157–166. https://doi.org/10.2166/wpt.2021.111.
27 Sonwani, R.K., Swain, G., Jaiswal, R.P., Singh, R.S., Rai, B.N., 2021. Moving bed biofilm reactor with immobilized low-density polyethylene–polypropylene for Congo red dye removal. Environ. Technol. Innov. 23, 101558 https://doi.org/10.1016/j.eti.2021.101558.
28 Swain, G., Maurya, K.L., Sonwani, R.K., Singh, R.S., Jaiswal, R.P., Rai, B.N., 2022. Effect of mixing intensity on biodegradation of phenol in a moving bed biofilm reactor: Process optimization and external mass transfer study. Bioresour. Technol. 351, 126921 https://doi.org/10.1016/j.biortech.2022.126921.
29 Thangaraj, S., Bankole, P.O., Sadasivam, S.K., Kumarvel, V., 2022. Biodegradation of Reactive Red 198 by textile effluent adapted microbial strains. Arch. Microbiol. 204 (1), 1–13. https://doi.org/10.1007/s00203-021-02608-9.
30 Tian, F., Wang, Y., Guo, G., Ding, K., Yang, F., Wang, H., Cao, Y., Liu, C., 2021. Enhanced azo dye biodegradation at high salinity by a halophilic bacterial consortium. Bioresour.Technol. 326, 124749 https://doi.org/10.1016/j.biortech.2021.124749.
31 Zhu, D., Ge, C., Sun, H., Wang, J., He, L., 2022. Bioremediation of tetramethyl thiuram disulfide and resource utilization of natural rubber wastewater by WR-2 Bacillus-dominated microbial community. Environ. Sci. Pollut. Res. 1–11 https://doi.org/10.1007/s11356-022-20267-1.
32 Zinatizadeh, A.A.L., Ghaytooli, E., 2015. Simultaneous nitrogen and carbon removal from wastewater at different operating conditions in a moving bed biofilm reactor (MBBR): process modeling and optimization. J. Taiwan Inst. Chem. Eng. 53, 98–111. https://doi.org/10.1016/j.jtice.2015.02.034.